$O(\alpha_s)$ Corrections to $b\bar{b} \to W^\pm H^\mp$ at the CERN Large Hadron Collider

Wolfgang Hollik and Shou-hua Zhu

Institut für Theoretische Physik, Universität Karlsruhe
D-76128 Karlsruhe, Germany

The $O(\alpha_s)$ corrections to the cross section for $b\bar{b} \to W^\pm H^\mp$ at the LHC are calculated in the minimal supersymmetric standard model (MSSM) in the $\overline{MS}$ and OS (on-mass-shell) renormalization schemes. The results in two schemes are in good agreement. In the $\overline{MS}$ scheme, the QCD corrections are negative and within $-14\% \sim -20\%$ for charged Higgs mass up to 1 TeV and $\tan\beta > 15$. For $\tan\beta = 2$, the magnitude of the QCD corrections can be greater than 30%.

1. The detection of Higgs particles is one of the most important objectives of the Large Hadron Collider (LHC). Charged Higgs bosons are predicted in extended versions of the Standard model (SM), like two-Higgs-doublet models (2HDM) and the Minimal Supersymmetric Standard Model (MSSM). A discovery of such an additional Higgs boson will immediately indicate physics beyond the SM; there is, hence, strong theoretical and experimental activity to provide the basis for its accurate exploration.

At hadron colliders, the charged Higgs boson $H^\pm$ could appear as the decay product of primarily produced top quarks if the mass of $H^\pm$ is smaller than $m_t - m_b$. For heavier $H^\pm$, other mechanism for $H^\pm$ production have been investigated: single Higgs-boson production associated with heavy quarks, like $gb \to H^- t$[1] and $qb \to q' b H^-$[2], and pair production of $H^\pm$ through tree-level $q\bar{q}$ annihilation and via the loop-induced gluon-fusion mechanism [3]. Moreover, single $H^\pm$production in association with a W boson, via tree-level $b\bar{b}$ annihilation and one-loop gg fusion has been proposed and analyzed [4]. Detailed studies [5] show that these production mechanisms at the LHC can help to explore the parameter space, even beyond $m_{H^\pm} \sim 1$TeV and down to at least $\tan\beta \sim 3$.

Since $b\bar{b}$ annihilation is the main source of the hadronic $W^\pm H^\mp$ production cross section, it is necessary to calculate and implement also the loop contributions to $b\bar{b} \to W^\pm H^\mp$ for more accurate theoretical predictions. Recently, the calculation of the $O(\alpha_{ew} m_{t(b)}^2/m_W^2)$ and $O(\alpha_{ew} m_{t(b)}^4/m_W^4)$ supersymmetric electroweak(EW) one-loop corrections were presented in [6] in the frame of the MSSM, which can give rise to a 10-15% reduction of the lowest-order result. In this paper, we deal with the one-loop QCD corrections to $b\bar{b} \to W^\pm H^\mp$.

2. The Feynman diagrams for charged Higgs-boson production via the parton process $b(p_1)\bar{b}(p_2) \to H^-(k_1)W^+(k_2)$, including the QCD corrections, can be found in Ref. [7]. We keep the finite b-quark mass throughout the calculation, in order to control the collinear divergences.

As usual, we define the Mandelstam variables as

$$\hat{s} = (p_1 + p_2)^2 = (k_1 + k_2)^2,$$
$$\hat{t} = (p_1 - k_1)^2 = (p_2 - k_2)^2,$$
$$\hat{u} = (p_1 - k_2)^2 = (p_2 - k_1)^2. \quad (1)$$

Taking into account the $O(\alpha_s)$ corrections, the renormalized amplitude for $b\bar{b} \to W^+H^-$ can be written in the following way,

$$\begin{aligned} M_{\rm ren} &= M_0^{(s)} + M_0^{(t)} + \delta\hat{M}^{V_1(s)}(H) + \delta\hat{M}^{V_1(s)}(h) + \delta\hat{M}^{V_1(s)}(A) \\ &\quad + \delta\hat{M}^{V_1(t)} + \delta\hat{M}^{S(t)} + \delta\hat{M}^{V_2(t)} + \delta M^{\rm box}. \end{aligned} \tag{2}$$

$M_0^{(s)}$ and $M_0^{(t)}$ are the s- and t-channel tree-level diagrams corresponding to Fig. 1(a) and Fig. 1(b), which are given by

$$\begin{aligned} M_0^{(s)} &= \frac{gh_b}{\sqrt{2}}\left[-\frac{\cos\alpha\sin(\alpha-\beta)}{\hat{s}-m_H^2} + \frac{\sin\alpha\cos(\alpha-\beta)}{\hat{s}-m_h^2}\right](M_5+M_6+M_9+M_{10}) \\ &\quad + \frac{gh_b\sin\beta}{\sqrt{2}\,(\hat{s}-m_A^2)}\,(M_5-M_6+M_9-M_{10})\,, \\ M_0^{(t)} &= \frac{g}{\sqrt{2}(\hat{t}-m_t^2)}\left[h_b\sin\beta(2M_9+m_bM_1+M_3) - h_tm_t\cos\beta M_2\right], \end{aligned} \tag{3}$$

where

$$h_b = \frac{gm_b}{\sqrt{2}m_W\cos\beta}\,, \quad h_t = \frac{gm_t}{\sqrt{2}m_W\sin\beta} \tag{4}$$

denote the Yukawa couplings of the bottom and top quarks. M_i are reduced standard matrix elements, which could be found in Ref. [7].

The terms $\delta\hat{M}$ in (2) describe the virtual contributions from the 2- and 3-point functions together with their counterterms, and $\delta M^{\rm box}$ denotes the contribution from the irreducible 4-point function. The vertex and self-energy corrections to the tree-level process are included in $\delta\hat{M}^{V,S}$, which are given by

$$\begin{aligned} \delta\hat{M}^{V_1(s)}(H,h) &= \frac{gh_b}{\sqrt{2}}[-\frac{\cos\alpha\sin(\alpha-\beta)}{\hat{s}-m_H^2}, \frac{\sin\alpha\cos(\alpha-\beta)}{\hat{s}-m_h^2}](M_5+M_6+M_9+M_{10}) \\ &\quad \times[\frac{\delta m_b}{m_b} + \frac{1}{2}\delta Z_L^b + \frac{1}{2}\delta Z_R^b] + \delta M^{V_1(s)}(H,h), \\ \delta\hat{M}^{V_1(s)}(A) &= \frac{gh_b\sin\beta}{\sqrt{2}(\hat{s}-m_A^2)}[\frac{\delta m_b}{m_b} + \frac{1}{2}\delta Z_L^b + \frac{1}{2}\delta Z_R^b](M_5-M_6+M_9-M_{10}) + \delta M^{V_1(s)}(A), \\ \delta\hat{M}^{V_1(t)} &= \frac{g}{\sqrt{2}(\hat{t}-m_t^2)}[h_b\sin\beta(2M_9+m_bM_1+M_3) - h_tm_t\cos\beta M_2] \\ &\quad \times(\frac{1}{2}\delta Z_L^t + \frac{1}{2}\delta Z_L^b) + \delta M^{V_1(t)}, \\ \delta\hat{M}^{S(t)} &= \frac{g}{\sqrt{2}(\hat{t}-m_t^2)^2}[h_b\sin\beta(2M_9+m_bM_1+M_3)(2m_t\delta m_t + (m_t^2-\hat{t})Z_L^t) \\ &\quad -h_t\cos\beta M_2(\delta m_t(m_t^2+\hat{t}) + m_t(m_t^2-\hat{t})Z_L^t)] + \delta M^{S(t)}, \\ \delta\hat{M}^{V_2(t)} &= \frac{g}{\sqrt{2}(\hat{t}-m_t^2)}[h_b\sin\beta(2M_9+m_bM_1+M_3)(\frac{\delta m_b}{m_b} + \frac{1}{2}Z_R^t + \frac{1}{2}Z_L^b) \\ &\quad -h_tm_t\cos\beta M_2(\frac{\delta m_t}{m_t} + \frac{1}{2}Z_L^t + \frac{1}{2}Z_R^b)] + \delta M^{V_2(t)}. \end{aligned} \tag{5}$$

Therein, $\delta M^{V_1(s)}(H,h,A)$, $\delta M^{V_1(t)}$, $\delta M^{S(t)}$, $\delta M^{V_2(t)}$ represent the unrenormalized one-loop corrections arising, respectively, from the $b\bar{b}H(h,A)$ vertex diagrams in Fig. 1(c), the

$\bar{t}bH^-$ vertex diagram Fig. 1(d), the $\bar{b}tW^+$ vertex diagram Fig. 1(e), and the top-quark self-energy diagram Fig. 1(f); $\delta M^{\rm box}$ corresponds to the box diagram Fig. 1(g). All the $\delta M^{V,S}$ and $\delta M^{\rm box}$ can be obtained in Ref. [7].

Here we present the analytical results in the $\overline{MS}$ scheme; accordingly, the quark masses in (4) are running masses $m_{b,t}(\mu)$. The results in the OS scheme can be easily obtained by using the pole masses and replacing the corresponding field- and mass-renormalization constants. Actually in the $\overline{MS}$ scheme, we must add the finite part of the wave-function renormalization constants for the b quarks, according to the LSZ prescription.

From the self-energy diagram in Fig. 1(h) for the b, t quarks we get the explicit expressions of the renormalization constants, valid for both the t and b quark,

$$\begin{aligned} \frac{\delta m}{m} &= -\frac{\alpha_s}{4\pi} 3C_F\Delta, \\ Z_L &= Z_R = -\frac{\alpha_s}{4\pi} C_F\Delta, \qquad \text{with} \\ \Delta &= \frac{2}{\epsilon} - \gamma_E + \log(4\pi), \quad \epsilon = 4 - D, \end{aligned} \tag{6}$$

in dimensional regularization.

After squaring the amplitude and performing the spin summations, we can get cross section for the process $b\bar{b} \to W^+H^-$ with virtual corrections.

3.The virtual corrections involve an infrared singularity from the massless gluon. For our purpose, we can use a small gluon mass λ for regularization, which allows to identify the infrared divergence as a $\log(\lambda)$ term. This infrared divergence is cancelled by adding the corresponding real-gluon-radiation corrections, displayed in Fig. 1(i-m). For technical reasons, it is convenient to perform the phase-space integration over a soft- and hard-gluon part separately. The soft-gluon contribution to the cross section at the partonic level is proportional to the tree-level cross section $\hat{\sigma}^0_{b\bar{b}\to H^\pm W^\mp}$ for $b\bar{b} \to H^\pm W^\mp$,

$$\begin{aligned} \hat{\sigma}^{\rm soft} &= \hat{\sigma}^0_{b\bar{b}\to H^\pm W^\mp}\, \delta_s\,, \\ \delta_s &= -C_F\frac{\alpha_s}{2\pi}\{\log\frac{4\Delta E^2}{\lambda^2} + \log\frac{m_b^2}{\hat{s}} + \log\frac{m_b^2}{\hat{s}}\log\frac{4\Delta E^2}{\lambda^2} + \frac{\pi^2}{3} + \frac{1}{2}\log^2(\frac{m_b^2}{\hat{s}})\}, \end{aligned} \tag{7}$$

where ΔE is the energy cutoff for soft gluons. After adding the cross section with the virtual corrections, the sum is independent on λ, and the $\log^2$ term cancels.

For the hard-gluon part, we use the Monte Carlo packages BASES [8] to perform the phase space integration, with the cutoff that the energy of the gluon is greater than ΔE. We do not give detailed expressions here. Numerically it was checked that the sum $\hat{\sigma}^{\rm soft} + \hat{\sigma}^{\rm hard}$ is independent of the cutoff ΔE.

At $O(\alpha_s)$, there are also initial-gluon contributions from $gb \to bW^\pm H^\mp$, the Feynman diagrams can be obtained from Fig. 1(i-m) by treating gluon and b quark as incoming partons. For the processes, we should caution how to subtract the on-shell top quark and/or charged Higgs boson contributions. Following the methods of Ref. [9], the partonic cross section after subtracting the on-shell contributions of subprocess $gb \to bW^\pm H^\mp$ can be written as:

$$\begin{aligned} \hat{\sigma}^{0,sub}_{gb\to bW^\pm H^\mp} &= \hat{\sigma}^0_{gb\to bW^\pm H^\mp} - \hat{\sigma}^0_{gb\to tH^-} Br(t\to bW^+) \\ &\quad -\hat{\sigma}^0_{gb\to tW^-} Br(t\to bH^+). \end{aligned} \tag{8}$$

The cross section of $g\bar{b} \to \bar{b}W^{\pm}H^{\mp}$ can be obtained similarly.

4. In the approach described above we have considered the real-gluon corrections, which give rise to a term involving $\log(\hat{s}/m_b^2)$ from the region where the b quark splits into a collinear b-quark–gluon pair and the gluon into a collinear b pair. This logarithm is already contained in the heavy-quark distribution function, hence it has to be removed. This can be done, following [10], by subtracting the tree-level process $b\bar{b} \to H^{\pm}W^{\mp}$ convoluted with one heavy-quark distribution function given by the perturbative solution to DGLAP equation,

$$\begin{aligned} \tilde{b}_{(bb)}(x,\mu_f) &= \frac{\alpha_s(\mu)}{2\pi}\log(\frac{\mu_f^2}{m_b^2})\int_x^1 \frac{dy}{y}P_{qq}(\frac{x}{y})b(y,\mu_f), \\ \tilde{b}_{(bg)}(x,\mu_f) &= \frac{\alpha_s(\mu)}{2\pi}\log(\frac{\mu_f^2}{m_b^2})\int_x^1 \frac{dy}{y}P_{qg}(\frac{x}{y})g(y,\mu_f), \end{aligned} \tag{9}$$

where

$$\begin{aligned} P_{qq}(z) &= C_F[\frac{1+z^2}{(1-z)_+}+\frac{3}{2}\delta(1-z)], \\ P_{qg}(z) &= \frac{1}{2}[z^2+(1-z)^2]. \end{aligned} \tag{10}$$

In this way, the total cross section at $O(\alpha_s)$ can be expressed as

$$\begin{aligned} \sigma^{NLO} = {} & \bar{b}\otimes\hat{\sigma}_{b\bar{b}}\otimes b - \tilde{b}_{(bb)}\otimes\hat{\sigma}^0_{\bar{b}b\to H^{\pm}W^{\mp}}\otimes b - \bar{b}\otimes\hat{\sigma}^0_{\bar{b}b\to H^{\pm}W^{\mp}}\otimes\tilde{b}_{(bb)} \\ & + b\otimes\hat{\sigma}^{0,sub}_{bg\to bH^{\pm}W^{\mp}}\otimes g - b\otimes\hat{\sigma}^0_{\bar{b}b\to H^{\pm}W^{\mp}}\otimes\tilde{b}_{(bg)} \\ & + \bar{b}\otimes\hat{\sigma}^{0,sub}_{\bar{b}g\to\bar{b}H^{\pm}W^{\mp}}\otimes g - \bar{b}\otimes\hat{\sigma}^0_{\bar{b}b\to H^{\pm}W^{\mp}}\otimes\tilde{b}_{(bg)}, \end{aligned} \tag{11}$$

where $\hat{\sigma}_{b\bar{b}}$ is the infrared-finite parton cross section which is given by the sum of $\hat{\sigma}^{\text{virt}} + \hat{\sigma}^{\text{soft}} + \hat{\sigma}^{\text{hard}}$. In eq. (11), $A\otimes\hat{\sigma}\otimes B$ represents the cross section of the subprocess $\hat{\sigma}$ is convoluted with the parton distribution functions (P DF) A and B,

$$A\otimes\hat{\sigma}\otimes B = \int_{z_0}^1 dz\,\frac{dL}{dz}\,\hat{\sigma}(z^2 s)\,, \quad z_0 = \frac{m_W + m_{H^-}}{\sqrt{s}}\,, \tag{12}$$

where $\sqrt{s}$ is the overall CM energy of the pp system, and the parton luminosity dL/dz is defined as

$$\frac{dL}{dz} = 2z\int_{z^2}^1 \frac{dx}{x}\,A(x,\mu_f)\,B(\frac{z^2}{x},\mu_f). \tag{13}$$

5. We now present a numerical discussion of the QCD corrections to $W^{\pm}H^{\mp}$ associated production at the LHC. The SM input parameters in our calculations were taken to be $\alpha_{ew}(m_Z) = 1/128.8$, $\alpha_s(m_Z) = 0.118$, $m_W = 80.41$GeV and $m_Z = 91.1867$GeV, and the pole masses of top and bottom quarks are $m_t = 175$GeV and $m_b = 4.7$GeV. We have used the two-loop running $\overline{MS}$ quark masses [11] and strong coupling constant [12], the CTEQ5M PDF [13], and we choose the factorization and renormalization scale as $m_{H^{\pm}} + m_W$, if not stated otherwise. The expressions given in the previous section are valid for a general Two-Higgs-doublet model; they cover the MSSM case for a specific choice of the Higgs-boson masses and mixing angles. Here we focus on the MSSM scenario, taking into account the one-loop relations [14] between the Higgs-boson masses $M_{h,H,A,H^{\mp}}$ and the angles α and β, with m_{H^+} and β chosen as the two independent Higgs-input parameters, together with $M_S = 1$ TeV as a genuine SUSY mass scale. As a remark, the SUSY-QCD corrections arising from virtual gluino and squarks may also become important for specific parameters, which will be studied separately.

Fig. 1 shows $\delta = (\sigma^{NLO} - \sigma^0)/\sigma^0$ as a function of m_{H^+}. As pointed out before, due to the competition between the top–Higgs and bottom–Higgs Yukawa couplings, the cross sections are relatively small for intermediate values of $\tan\beta$, around $\tan\beta \sim 6$ (see Fig. 6). From the figures, we can see that the QCD corrections are negative and the magnitude is greater than 14% for all charged Higgs mass and $\tan\beta$. For $\tan\beta = 2$, the QCD corrections can decrease the cross section more than 30%. Table 1 contains numerical results for the relative correction δ for a low and a high value of $\tan\beta$, $\tan\beta = 2$ and 50.

Fig. 2 the relative correction δ as a function of $\tan\beta$, for $m_{H^\pm} = 200, 500$ and 1000 GeV. From the figures, one can see that the QCD corrections are almost independent of $\tan\beta$ when $\tan\beta > 15$. For $\tan\beta < 15$, the magnitude of the QCD corrections decreases with the increment of $\tan\beta$.

6. To summarize, in the $\overline{MS}$ scheme, the QCD corrections are negative and within $-14\% \sim -20\%$ for charged Higgs mass up to 1 TeV and $\tan\beta > 15$. For $\tan\beta = 2$, the magnitude of the QCD corrections can be greater than 30%.

The analytical results given in this paper are also valid in a general 2-Higgs-doublet model, where the constrains among Higgs masses and angles α and β are released. As a final remark, the higher-order contributions arising from the $gg \to H^\pm W^\mp b\bar{b}$, may also be important, especially for lower values of the charged Higgs-boson mass. They are presently under investigation.

References

[1] J.F. Gunion, H.E. Haber, F.E. Paige, W.-K. Tung and S.S.D. Willenbrock, Nucl. Phys. **B294** 621 (1987); C.S. Huang and S.H. Zhu, Phys. Rev. D60, 075012 (1999); L. G. Jin, C. S. Li, R. J. Oakes and S. H. Zhu, Phys. Rev. D **62**, 053008 (2000) [arXiv:hep-ph/0003159]; ibid, Eur. Phys. J. C **14**, 91 (2000) [arXiv:hep-ph/9907482].

[2] S. Morreti and K. Odagiri, Phys. Rev. **D55** 5627 (1997).

[3] E. Eichten, I. Hinchliffe, K. Lane and C. Quigg, Rev. Mod. Phys. **56** (1984) 579. A. Krause, T. Plehn, M. Spira and P. M. Zerwas, Nucl. Phys. **B519** (1998) 85; A. A. Barrientos Bendezu and B. A. Kniehl, Nucl. Phys. **B568** (2000) 305; O. Brein and W. Hollik, Eur. Phys. J. **C13** (2000) 175.

[4] D.A. Dicus, J.L.Hewett, C. Kao, and T.G. Rizzo, Phys. Rev. **D40**, 789 (1989); A.A. Barrientos Bendezu and B.A. Kniehl, Phys. Rev. **D59**, 015009 (1999); ibid, **D63**, 015009 (2001); O. Brein, W. Hollik and S. Kanemura, Phys. Rev. **D63**, 095001 (2001).

$m_{H^\pm}$ (GeV)	$\tan\beta = 50$	$\tan\beta = 2$
200	$\sim$ -16%	$\sim$ -32 %
500	$\sim$ -15%	$\sim$ -34 %
1000	$\sim$ -14%	$\sim$ -30 %

Table 1: QCD corrections to the process $b\bar{b} \to H^\pm W^\mp$ in MSSM and 2HDM in $\overline{MS}$ scheme. The renormalization and factorization scales are taken as $m_{H^\pm} + m_W$.

[5] S. Moretti and K. Odagiri, Phys. Rev. **D59**, 055008(1999); K. Odagiri, hep-ph/9901432; Phys. Lett. **B452**, 327(1999); D.P. Roy, Phys. Lett. **B459**, 607 (1999); S. Raychaudhuri and D.P. Roy, Phys. Rev. **D53**, 4902 (1996); M. Beneke, *et al*, hep-ph/0003033, in "Proceedings of the Workshop on Standard Model Physics (and More) at the LHC", CERN 2000-004, eds. G. Altarelli and M. Mangano.

[6] Y.S. Yang, C.S. Li, L.G. Jin and S.H. Zhu, Phys.Rev. D62 (2000) 095012.

[7] Wolfgang Hollik and Shouhua Zhu, Phys.Rev.D65:075015,2002.

[8] S. Kawabata, Comput. Phys. Commun. 88, 309 (1995).

[9] For example to see, S.H. Zhu, hep-ph/0109269, to appear in Phys. Lett. B; T. M. Tait, Phys. Rev. D **61**, 034001 (2000) [hep-ph/9909352].

[10] See for examples, D.A. Dicus, T. Stelzer, Z. sullivan and S. Willenbrock, Phys. Rev. D59, 094016 (2000) and references therein.

[11] J. Vermaseren, S. Larin and T. Ritbergen, Phys. Lett. **B405** , 327 (1997).

[12] Particle Data Group, Eur. Phys.J. C 3, 1 (1998).

[13] H.L. Lai, *et al.*(CTEQ collaboration), Eur. Phys.J. C 12 (2000) 375.

[14] A. Dabelstein, Ph.D. thesis, Munich, 1993, MPI-Ph/93-64; A. Dabelstein, Z. Phys **C 67**,495 (1995); M. Spira, Fortsch. Phys. 46 (1998) 203.

[15] G. J. van Oldenborgh and J. A. Vermaseren, Z. Phys. C **46**, 425 (1990).

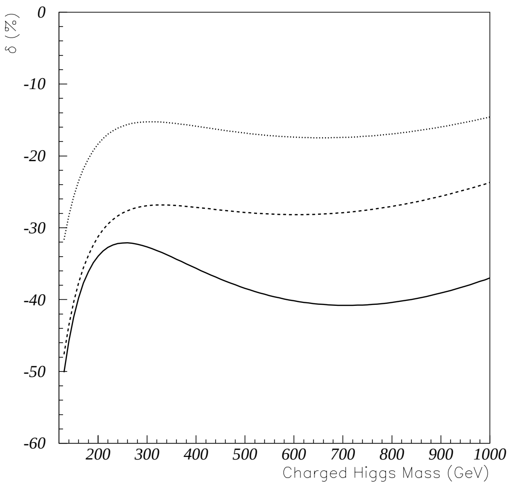

Figure 1: The QCD relative corrections to the cross sections for the subprocesses $b\bar{b} \to H^{\pm}W^{\mp}$ and $gb(\bar{b}) \to H^{\pm}W^{\mp}b(\bar{b})$ versus $m_{H^{\pm}}$. The lines correspond to $\tan\beta = 2$(solid), 6(dashed) and 50(dotted).

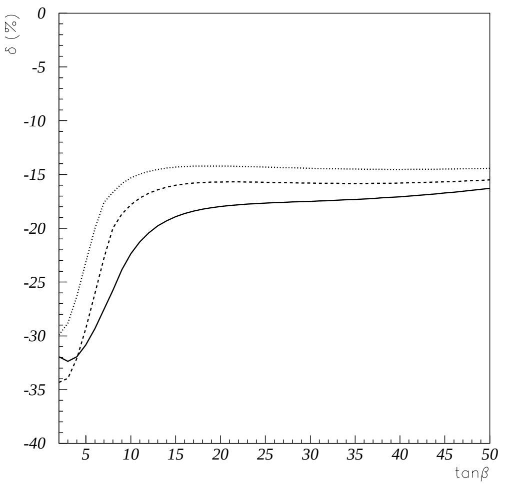

Figure 2: Same as Fig. 1 except versus $\tan\beta$. The lines correspond to $m_{H^{\pm}} = 200$(solid), 500(dashed) and 1000 GeV (dotted).